

Electrostatic versus polarization effects in the adsorption of aromatic molecules of varied polarity on an insulating hydrophobic surface

This article has been downloaded from IOPscience. Please scroll down to see the full text article.

2008 J. Phys.: Condens. Matter 20 035215

(<http://iopscience.iop.org/0953-8984/20/3/035215>)

View [the table of contents for this issue](#), or go to the [journal homepage](#) for more

Download details:

IP Address: 129.252.86.83

The article was downloaded on 29/05/2010 at 07:26

Please note that [terms and conditions apply](#).

Electrostatic versus polarization effects in the adsorption of aromatic molecules of varied polarity on an insulating hydrophobic surface

Kat F Austen^{1,4}, Toby O H White¹, Arnaud Marmier^{2,5},
Steve C Parker^{2,3}, Emilio Artacho¹ and Martin T Dove¹

¹ Department of Earth Science, University of Cambridge, Cambridge CB1 2PF, UK

² School of Engineering, Computing and Mathematics, University of Exeter, Exeter EX4 4QF, UK

³ Department of Chemistry, University of Bath, Bath Spa, BA2 7AY, UK

E-mail: kfa20@cam.ac.uk

Received 6 August 2007, in final form 12 November 2007

Published 19 December 2007

Online at stacks.iop.org/JPhysCM/20/035215

Abstract

Ab initio calculations have been used to investigate the electronic and energetic behaviour accompanying the adsorption of aromatic molecules of different polarities onto an insulating hydrophobic surface, as a convenient model for the study of characteristic weak adsorption processes in biochemistry (ligand–receptor interactions) and geochemistry (aromatic pollutants on soil minerals). Four poly-chlorinated dibenzo-*p*-dioxin molecules of different polarities were chosen as adsorbates; the surface was the (001) surface of pyrophyllite, a chemically inert, weakly polar, covalently bonded surface. The fairly weak interactions were observed to be dominated by local electrostatics rather than global multipoles or hybridization. The polarization induced on the adsorbate has been analysed. A small transfer of electron density was also observed from the molecule to the surface.

(Some figures in this article are in colour only in the electronic version)

1. Introduction

The non-bonding interaction between partly ionic systems and aromatic compounds that possess a variety of polarities due to their substituent groups represents an important common theme in biochemistry (ligand–receptor interactions), geochemistry (organic matter in the soil) and biogeochemistry. Despite the importance of detailed atomistic knowledge for extended systems of this type, data is quite limited due to the complexities encountered in studying these systems using both experimental and computational techniques. This work aims to elucidate the electronic nature of the weak interactions that arise between these organic molecules and hydrophobic

surfaces, and how these vary with different distributions of polarity in the molecules.

This work reports calculations carried out on a model system that is, on the one hand, rich enough to capture the subtleties of the interactions together with the frustration of multiple docking possibilities, while on the other hand is simple enough to be amenable to systematic theoretical atomistic studies. Polychlorinated dibenzo-*p*-dioxins (PCDDs) have been selected as adsorbates. There are 76 different congeners of the PCDD molecule, originating from the number and disposition of chlorine substitution at any hydrogen site on the molecule (see figure 1). PCDD molecules are, predominantly, present in the environment due to release of these chemicals after their use in industry during the latter part of the last century. PCDDs are toxic, and their toxicity varies with chlorine number and distribution across the molecule; it

⁴ Author to whom any correspondence should be addressed.

⁵ Formerly at Department of Chemistry, University of Bath, Bath Spa BA2 7AY, UK.

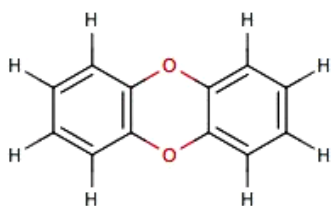


Figure 1. Dibenzo-*p*-dioxin. Any H can be replaced by Cl in any configuration to create 76 different molecules.

can be postulated that their behaviour at surfaces may vary in a similar manner.

As the substrate, the (001) surface of the mineral pyrophyllite ($\text{Al}_4\text{Si}_8\text{O}_{20}(\text{OH})_4$) has been chosen. The surface is simple, very flat and chemically inert, with small partial ionicity in its surface Si–O bonds. As such, the surface is hydrophobic in character, and provides an excellent lead-in to understanding weak adsorption reactions. In a case such as this, it is not intuitively obvious what will be the preferred position of adsorption on the surface, or what will be the variation of the energy with respect to position.

Experimentally, adsorption energies for PCDDs are very hard to obtain, as they have a very low vapour pressure, which may explain the lack of experimental results currently available for the system [1]. There has been work on related systems, for example benzene adsorption on palygorskite [2], but these are few and far between. The system is also difficult to deal with computationally, due to the nature of the energy landscape and the large number of different PCDD molecules available for study. This work presents results for four PCDD molecules, which have different numbers and dispositions of chlorine atoms. The adsorption of the molecules has been studied at the density functional theory (DFT) level, and the results provide information on the mode of adsorption and the electronic changes on adsorption.

2. Methodology

The energy landscape of the system has been explored as part of an associated study that looked at the application of different computational methods to this problem [3]. Empirical potential calculations were carried out by scanning the molecules across the pyrophyllite (001) surface, in order to determine the energy landscape. Once the lowest energy geometry had been found, these configurations were optimized using DFT methods and an in-depth analysis of the results is reported here, focusing on the chemical and physical interactions between the surface and adsorbate.

All calculations were performed using the generalized gradient approximation (GGA) PBE (Perdew, Burke and Ernzerhof) functional [4]. It has been shown that, of the GGA functionals tested, the PBE functional performed best for analogous systems containing weak interactions. Additionally, PBE performed better than most hybrid and meta GGA functionals, including the B3LYP hybrid functional [5]. It is known that dispersive interactions are strictly absent from GGA calculations; this effect will be discussed below.

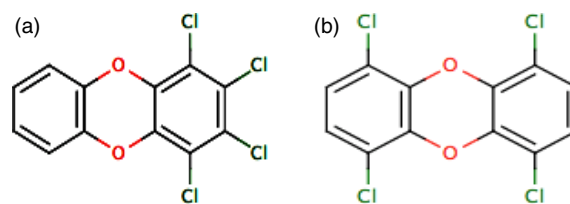


Figure 2. (a) PCDD with large dipole (4CDD-1), (b) PCDD with no dipole (4CDD-2), both used in this study.

Full geometry optimizations were carried out on the chosen four molecules: the fully protonated (hereafter referred to as 0CDD) and fully chlorinated (8CDD) molecules and two intermediates. The intermediate molecules both had four Cl and four H atoms on the phenyl rings, one arranged to give the largest possible dipole (4CDD-1), the other to give no dipole (4CDD-2) within the molecule (figure 2).

Both the calculation of the electron density at each step and the minimization algorithm required tight tolerances to have reached adequate convergence, as the interactions between the organic molecules and the clay surface were found to be weak. A mesh cutoff of 250 Ryd was used for the integrals in real space, the tolerance for self-consistency was designated as 5×10^{-5} , and a force tolerance of $10 \text{ meV } \text{\AA}^{-1}$ was used.

Pyrophyllite is a layer silicate and has a sheet-like structure, each layer being made up of octahedrally coordinated Al atoms sandwiched between tetrahedrally coordinated Si atoms. The total layer has a depth of approximately 17 \AA , and is seven atomic layers thick. A 4×2 supercell of one layer's thickness was used for the pyrophyllite surface slab, measuring $21 \text{ \AA} \times 18 \text{ \AA}$ laterally and comprised of 320 atoms. A vacuum gap of 25 \AA was used between surface slabs, large enough to prevent interactions between the molecule above the surface and the underside of the surface's periodic image. Given the use of a large supercell in the calculations, and the insulating nature of the material, it was considered adequate to use the Γ point ($k = 0$) for k -sampling.

The SIESTA method [6] has been used in this work. It uses norm-conserving pseudopotentials to describe the inner electrons of the atoms within the system, the outer orbitals being described by atom centred basis sets. In this work, Troullier–Martins pseudopotentials were used. A double-zeta polarized basis set was used throughout, as obtained variationally [7] in various reference systems at 0.2 GPa [7–10]. The basis set superposition error (BSSE), characteristic of atom centred basis set DFT methods, has been found to be small in these systems for these basis sets. The BSSE was found to be an order of magnitude smaller than the associated counterpoise correction for the basis sets used [11]; therefore counterpoise corrections are not included in the calculation of adsorption energies. A fuller discussion of these results is beyond the scope of this work, but will be presented as part of a larger, associated study that addresses the issue in detail [11]. In all cases the adsorption energy has been calculated in the usual way: $U_{\text{adsorption}} = U_{\text{molecule+surface}} -$

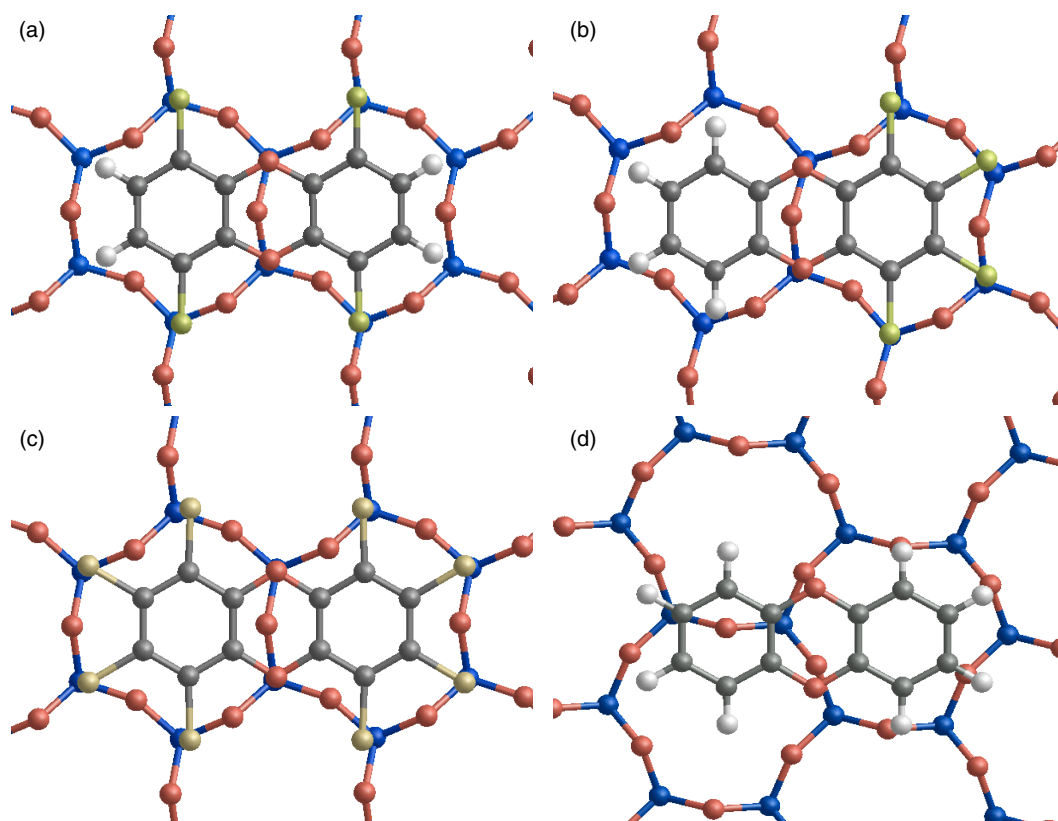


Figure 3. Adsorption geometries for (a) 4CDD-2, (b) 4CDD-1, (c) 0CDD and (d) 8CDD on the pyrophyllite surface, shown from above.

($U_{\text{molecule}} + U_{\text{surface}}$), where U is the internal energy of the system.

3. Results and discussion

3.1. Adsorption geometry

Figure 3 shows the adsorption configurations for the four molecules studied. Each molecule that contains chlorine lies preferentially over two surface Si–O hexagons, the Cl atoms interacting with the surface Si atoms; this is the most favourable configuration for the fully chlorinated molecule. This configuration is obviously not as favourable for the fully protonated dioxin molecule, which shows preferential interactions between H atoms and surface O atoms. It appears that the strongest interactions in this case, therefore, are the interactions between the phenyl ring substituents and the Si or O of the surface hexagons. Secondary to this is the preference for the dioxin oxygen atoms to sit above the Si atoms in an Si–O–Si bridge, and for surface O atoms to sit at the centre of the molecule's rings.

It is clear that the influence of the Cl atoms dominates the adsorption, dictating the disposition of the molecule on the surface by being located on top of Si atoms. The 8CDD molecule fits perfectly on top of two silica rings. The 0CDD molecule uses H-bonds to adsorb, but can only do so for one ring. For the partially chlorinated molecules, Si–Cl interactions dominate over H-bonds. It is, however, important to note that the differences in disposition, and to a lesser extent

Table 1. Adsorption energies calculated with DFT for four PCDD molecules, the fully chlorinated (8CDD), fully protonated (0CDD) and two intermediates—one with a large dipole (4CDD-1) and one with no dipole (4CDD-2).

	0CDD	4CDD-1	4CDD-2	8CDD
Adsorption energy (eV)	−0.44	−0.47	−0.47	−0.51

chlorination, have only a secondary effect on the adsorption energy [3].

3.2. Adsorption energy

Once the coordinates of each system had been relaxed, the adsorption energies were calculated (table 1). They show that the fully chlorinated molecule adsorbs more strongly than the fully protonated molecule.

As mentioned previously, the interaction between the molecule and the surface is weak, suggesting shallow potential energy landscapes. When comparing the final geometries with those obtained using empirical force fields [3], which were used as starting points, the geometries changed only slightly during the minimization; the DFT optimization does not significantly change the position of the molecule in relation to the surface. The largest displacement of the molecule above the surface is approximately 0.4 Å. While this is large compared to the intermolecular distances, the value is small when compared to the displacement of the molecule in

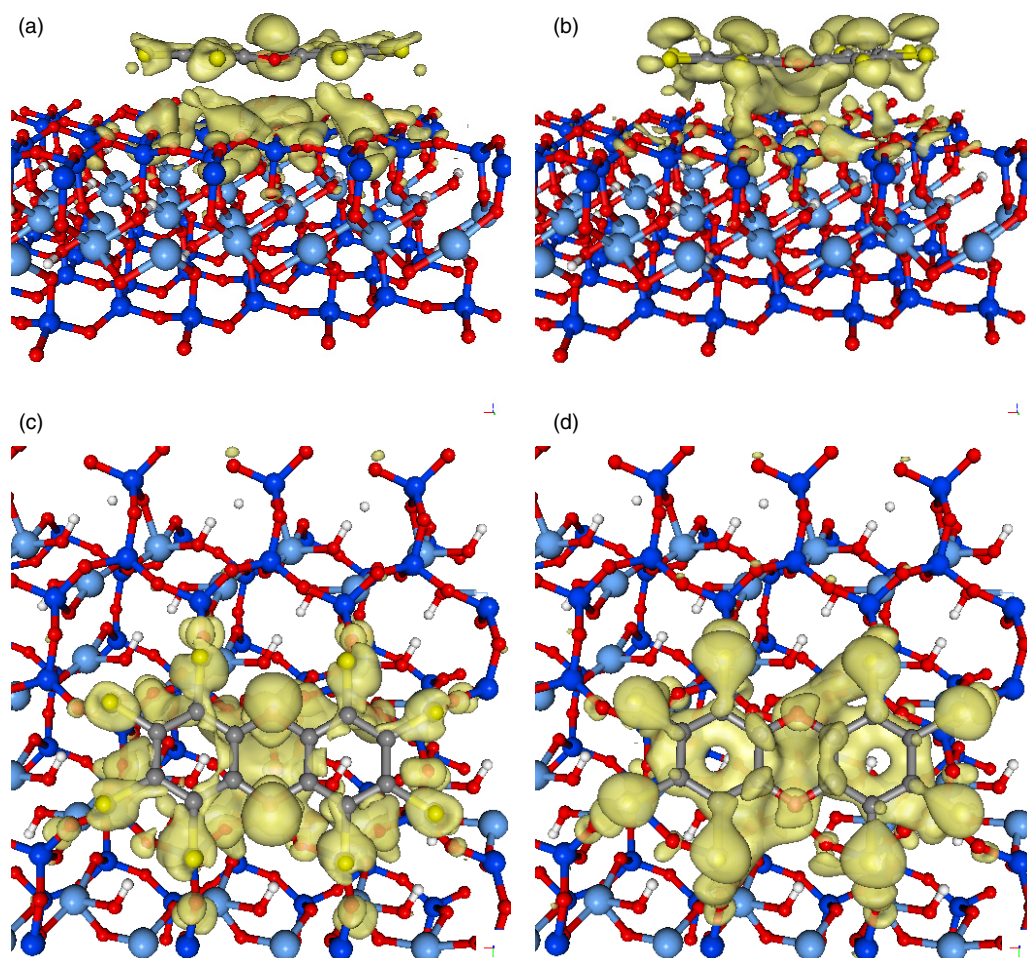


Figure 4. Plots showing from the side ((a), (b)) and from above ((c), (d)), the difference in the electron density of the adsorbed 8CDD system when compared with the electron densities of the non-interacting molecule and surface. A value of $\Delta\rho = 0.0001e^-/\text{Bohr}^3$ was chosen for clarity of representation. (a), (c) Gain of electron density, (b), (d) loss of electron density.

relation to the surface, as the height of the molecule above the surface is 3.8 Å. The smallness of the displacements from the original geometries is somewhat surprising, since the charge redistribution in the molecules is far from trivial. This aspect of adsorption is only partially captured by the use of force fields. The electron distribution and redistribution is discussed below.

3.3. Electron density changes on adsorption

An examination of figures 4 and 5 shows that the general trend is for a loss of electron density on the molecule and a gain of electron density by the surface. Additionally, it appears that the increase in electron density goes to anti-bonding states, suggesting that enhanced polarization leads to a predominantly electrostatic interaction between the molecule and the surface. Furthermore, both for the 8CDD and the 0CDD, the π -delocalized electron densities on the phenyl rings are very much diminished upon adsorption. This is especially the case for the 0CDD molecule, where both the upper and lower delocalized orbital electron densities are affected. In the case of 0CDD, it seems that in compensation for this the σ -bonds between the carbon atoms in the phenyl rings gain electron density on adsorption.

Table 2. Average Voronoi charges on the molecular atoms with and without the presence of the surface.

0CDD	Without surface	At surface
C	-0.026	-0.019
C near O	0.132	0.138
H	0.041	0.049
O	-0.324	-0.319
<hr/>		
8CDD		
C	0.135	0.138
C near O	0.144	0.150
O	-0.240	-0.249
Cl	-0.145	-0.140

The dioxin oxygen atoms gain charge in outer regions, losing it from regions closer to the nucleus. Analysis of both the Mulliken and Voronoi [12] charges for the adsorbed and free molecules shows a net transfer of charge from the molecule to the surface on adsorption (table 2). The overall transfer calculated by the Voronoi method is $0.1e^-$ for the 8CDD molecule and $0.15e^-$ for 0CDD, in agreement with the trend in Mulliken charges, which show a charge transfer on adsorption of $0.06e^-$ and $0.09e^-$, respectively. These changes,

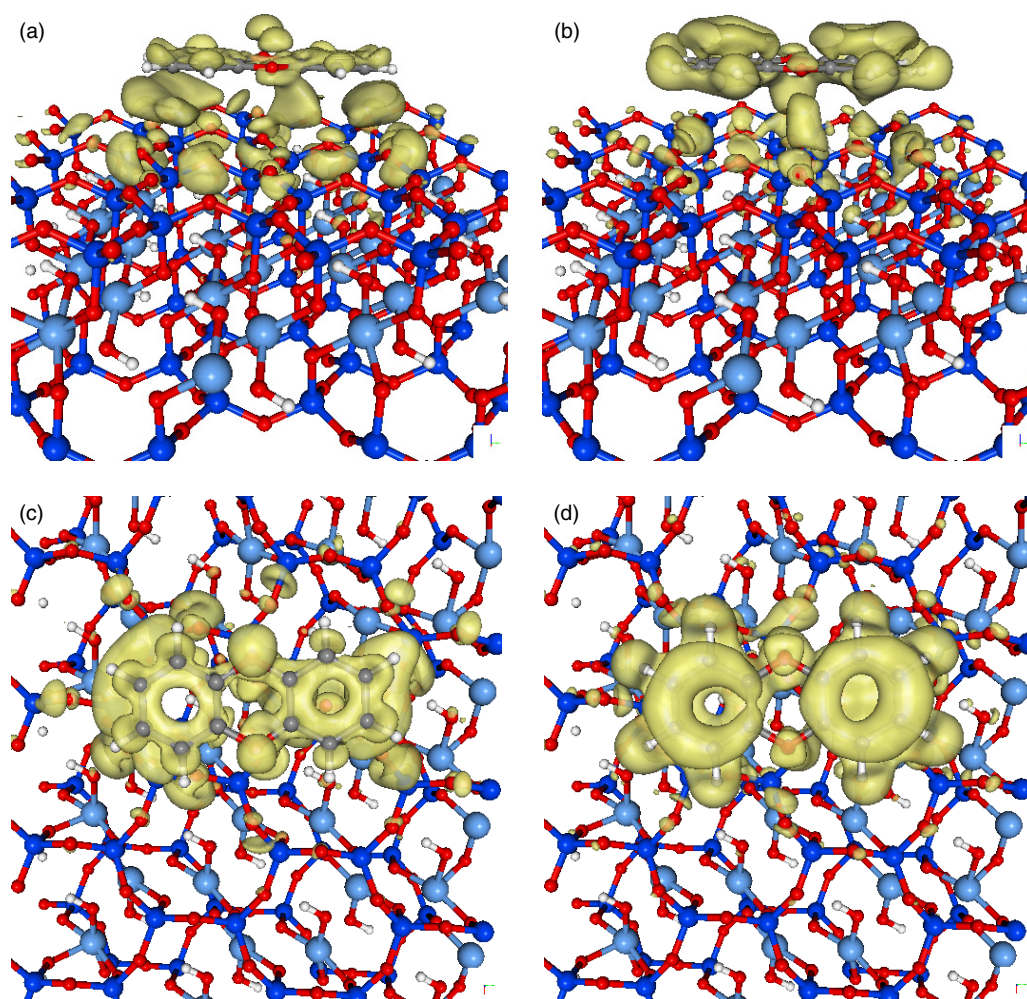


Figure 5. (As in figure 4 for 8CDD) Plots showing from the side ((a), (b)) and from above ((c), (d)), the difference in the electron density of the adsorbed 0CDD system when compared with the electron densities of the non-interacting molecule and surface. A value of $\Delta\rho = 0.0001e^-/\text{Bohr}^3$ was chosen for clarity of representation. (a), (c) Gain of electron density, (b), (d) loss of electron density.

though small, will nonetheless have an effect on the energy of adsorption, such that to a small extent there is a chemical contribution to the adsorption mechanism.

The majority of the charge is transferred to the surface oxygen atoms in the case of both molecules, with only a small net gain on the surface silicon and hydrogen atoms. The transferred charge from both the 0CDD and 8CDD molecules resides on the surface oxygen atoms immediately below the molecule. Proportionally, these oxygen atoms gain 1–4% of their initial Voronoi charge of approximately -0.4 . There is one oxygen atom that gains even more charge, 6% of its initial charge, and this is the oxygen atom that lies under the centre of the dioxin ring of each molecule, and the other high percentages of electron density gain are on oxygen atoms nearest this central dioxin ring.

Analysis of the Voronoi charges per atom shows that the greatest loss of electron density is from the oxygen atoms of the 8CDD molecule, losing $0.009e^-$ each, which is approximately 1% of the total oxygen atom charge. However, there are only two oxygen atoms per molecule, so the greatest total loss is from the carbon atoms, which lose $0.47e^-$ overall, split almost equally between the two phenyl rings, the greatest

loss sustained from the carbon atoms directly bonded to the central oxygen atoms of the molecule, which lose an average of $0.006e^-$ each, compared to the overall average of $0.004e^-$. As noted previously, examination of figure 4 shows that this loss is from the delocalized π -orbitals on the phenyl rings. It should be noted, however, that the values discussed here relate to very small changes in the electron density, and are not expected to cause an appreciable change in the chemical behaviour of the PCDD molecule. The chlorine atoms of the 8CDD molecule lose, on average, $0.005e^-$, corresponding to a net loss of $0.043e^-$, which is a number close to the net loss of the carbon atoms but spread over fewer atoms. Figure 4 indicates that the electron density lost from the chlorine atoms comes mainly from the Cl–C bonding orbitals, though some of this loss is compensated by polarization of the electron density into chlorine valence orbitals, shown clearly in figure 4(a).

The analysis of the Mulliken orbital populations shows that there is universally a small gain in electron density in the 3s orbital of the chlorine atoms on adsorption, and a much larger loss of electron density from the 3p orbitals, especially the $3p_z$. The Mulliken charges are mostly in accordance with the trends from the Voronoi charges for the changes relating to the

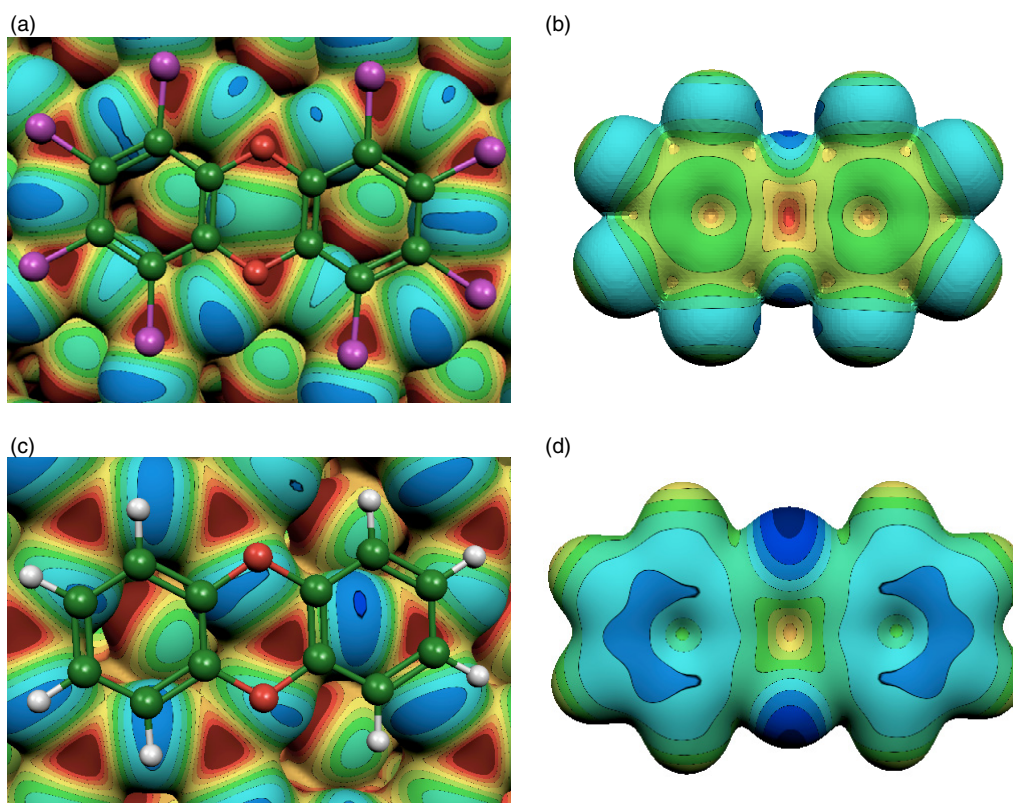


Figure 6. Electrostatic potential of the surface showing a ball and stick representation of the adsorption position of the (a) 8CDD, (c) 0CDD molecules. The electrostatic potential of the molecule is shown for (b) 8CDD and (d) 0CDD. Upper relief is negative electrostatic potential (blue in the online colour image), lower relief tends to be positive electrostatic potential (red in the online colour image). The darker the colour the larger the magnitude of the potential. The electrostatic potential has been projected on an electron density of $0.01e^-/\text{Bohr}^3$ for clarity.

carbon atoms of the molecule, with the most charge being lost from the carbon atoms directly bonded to oxygen. However, the Mulliken charges suggest that the next two carbon atoms, rather than losing less charge as indicated by the Voronoi charges, actually gain charge on adsorption. As it has been found previously that Voronoi charges are more independent of the basis set [12], combined with the electron density changes shown in figure 4, it is more likely that these carbon atoms also lose charge on adsorption.

It has already been mentioned that the electron density lost from the 0CDD molecule is mainly from the delocalized orbitals above and below the phenyl rings. From analysis of the Mulliken orbital populations there is some small gain in the 2p orbitals supplied by the H basis set within the calculation, and a much larger loss in electron density from the 1s orbitals of each H atom on adsorption; the numbers correspond well with the electron density plots shown in figure 5. From the Voronoi charges, there is a great deal more charge transferred from the phenyl ring that lies above the Si–O–Si bridge (right-hand ring of the molecule in figure 5) than there was from the ring above the surface Si–O ring, 0.049 compared to 0.033. Proportionally, the carbons from the ring above the bridge lose between 30 and 50% of their charge on adsorption (table 2), with the exception of those carbons directly bonded to the dioxin oxygen atoms, which already carry a positive charge and lose only 6% of their charge. By comparison, those carbons above the surface ring lose only 20% and 4% of their charge,

respectively. It can be concluded that the surface environment has a quantifiable influence on the molecular electron density upon adsorption.

3.4. Electrostatic potential of the system

After analysing the polarization of the system upon adsorption, the bare electrostatics are addressed, and for this purpose the electrostatic potential is shown in figure 6. The plot clearly shows that, for the 8CDD molecule, the most important electrostatic interactions are between the Cl atoms on the molecule and the Si atoms on the surface combined with the interaction between the oxygen atoms on the molecule and the silicon atoms on the surface, as seen in the geometry. To a lesser extent there will be a contribution from the positive electrostatic potential at the centre of the dioxin ring with the negative potential on the surface oxygen below it. From examination of the analogous diagram for 0CDD, it can be observed that there is no electrostatic contribution from the central dioxin ring to the geometry of adsorption in this case. The favourable interactions can be seen to be those between the hydrogen atoms, especially on the left-hand ring, and the surface oxygen atoms, which govern the adsorption geometry. There is an additional favourable interaction between the negative electrostatic potential on the outer part of the phenyl ring on the right-hand side and the positive electrostatic potential of the Si atom below it. It has been shown previously

from the Voronoi charges that this phenyl ring loses some charge to the oxygen atom in the centre of the ring, which can be observed from examination of the electrostatic potential shown of the surface below the 0CDD molecule in figure 6.

It is interesting to note that the previous analysis is all based on local electrostatic interactions between neighbouring atoms, and no reference is needed to longer range electrostatics. In fact, 4CDD-1 maximizes the electric dipole, while the reverse is true for 4CDD-2, and this difference has very little consequence on the magnitude of the binding energies.

4. Conclusions

The adsorption behaviour of a selection of PCDD molecules has been investigated using *ab initio* techniques in order to elucidate the nature of the chemical changes occurring on adsorption to a hydrophobic surface, that of pyrophyllite. The adsorption energies show increasing strength of adsorption with increasing number of chlorine atoms on the molecule. It has been observed that the inclusion of any chlorine atoms in the molecule changes the adsorption geometry, favouring a double docking above the hexagonal surface rings and maximizing the electrostatic interactions between the molecule's chlorine atoms and the Si atoms of the surface, and maximizing the favourable interactions between the latter and the oxygen atoms of the dioxin ring.

Overall there is a small change in the electron density on adsorption, but not so much as to greatly affect the chemistry of the molecule. For both end-member molecules, the changes in electron density on adsorption are increased in the population of anti-bonding molecular orbitals and polarization of bonds in the molecules. In the case of 0CDD especially, there is loss from the delocalized π -bonds and an increase in the density of the σ -bonds of the phenyl rings. On adsorption there is movement of the electron density to anti-bonding molecular orbitals, confirming the predominance of physisorption as the adsorption mechanism. The main contribution to adsorption is via electrostatic interactions, which are enhanced by polarization of bonds as the molecule and surface come into close proximity. The dominance of the electrostatic interactions, in combination with the change in adsorption geometry on the incorporation of Cl atoms into the molecule, helps explain why increasing the number of Cl atoms on the molecule will strengthen the binding between the molecule and the surface.

As mentioned previously, DFT methods do not include contributions from the dispersion interaction. The effect that this has on the adsorption energy has been discussed previously [3]. The aim of the current work is to determine whether the interaction most relevant to adsorption in the type of system studied here is polar interaction (whether moments or local), polarization or hybridization. It is not feasible to evaluate the inclusion of dispersion interactions on such

large systems with current computational capacity. However, investigation of this problem is the focus of current work and will be addressed in analogous systems in [11], where dispersion is included in the calculations using MP2 methods.

Acknowledgments

The authors wish to thank NERC for funding (NER/T/S/2001/00855, NE/C515698/1 and NE/C515704/1), and Jon Wakelin for his preliminary work on this system. The calculations were performed on the computers of the North West Grid, using *escience* tools of the eMinerals project. The authors would like to gratefully acknowledge Richard Bruin and Rik Tyer for generation of and help with using these tools.

References

- [1] Eitzer B D and Hites R A 1989 Polychlorinated dibenzo-para-dioxins and dibenzofurans in the ambient atmosphere of Bloomington, Indiana *Environ. Sci. Technol.* **23** 1389–95
- [2] Zhukova A I, Bondarenko S V and Tarasevich Y I 1976 Study of selectivity of natural sorbents with respect to hydrocarbons *Ukr. Khim. Zh.* **42** 708–11
- [3] Austen K F, Marmier A, White T O H, Parker S C, Dove M T and Artacho E 2007 Adsorption of dibenzo-*p*-dioxins on pyrophyllite: a two-pronged approach, in preparation
- [4] Perdew J P, Burke K and Ernzerhof M 1996 Generalized gradient approximation made simple *Phys. Rev. Lett.* **77** 3865–8
- [5] Zhao Y and Truhlar D G 2005 Benchmark databases for nonbonded interactions and their use to test density functional theory *J. Chem. Theor. Comput.* **1** 415–432
- [6] Soler J M, Artacho E, Gale J D, Garcia A, Junquera J, Ordejon P and Sanchez-Portal D 2002 The SIESTA method for *ab initio* order-*N* materials simulation *J. Phys.: Condens. Matter* **14** 2745–79
- [7] Anglada E, Soler J M, Junquera J and Artacho E 2002 Systematic generation of finite-range atomic basis sets for linear-scaling calculations *Phys. Rev. B* **66** 205101
- [8] Fernandez-Serra M V, Junquera J, Jelsch C, Lecomte C and Artacho E 2000 Electron density in the peptide bonds of crambin *Solid State Commun.* **116** 395–400
- [9] Junquera J, Paz O, Sanchez-Portal D and Artacho E 2001 Numerical atomic orbitals for linear-scaling calculations *Phys. Rev. B* **64** 235111
- [10] Paglia G, Rohl A L, Buckley C E and Gale J D 2005 Determination of the structure of gamma-alumina from interatomic potential and first-principles calculations: the requirement of significant numbers of nonspinel positions to achieve an accurate structural model *Phys. Rev. B* **71** 224115
- [11] Austen K F, Artacho E and Dove M T 2007 Comparison of methods used on the weak interactions arising in calculations of aromatic hydrocarbon compound adsorption on surfaces, in preparation
- [12] Fonseca Guerra C, Handgraaf J-W, Baerends E J and Bickelhaupt F M 2004 Voronoi deformation density (VDD) charges: assessment of the Mulliken, Bader, Hirshfeld, Weinhold, and VDD methods for charge analysis *J. Comput. Chem.* **25** 189–210